Journal of Functional Materials and Applied Engineering

Review Paper

Research Progress on Small Molecule Adsorbents for Direct Air Capture of Carbon Dioxide (CO_2)

Marcus Marru[1], Marlon Abeysinghe[2,*]

[1] School of Public Health, Department of Health Policy and Administration, Doctor of Public Health Leadership Program, University of Illinois Chicago, Chicago, Illinois, USA)
[2] Molecular Plant Biology, Department of Biochemistry and Food Chemistry, University of Turku, Turku, Finland
*Corresponding author: mamato2@uic.edu ; MAbe@mac.com

Abstract. Carbon capture and storage represents a pivotal strategy for mitigating atmospheric CO_2 accumulation and stabilizing global surface temperatures. Given the low volumetric concentration of CO_2 in ambient air (~0.415‰) and the high energy penalty associated with conventional adsorption processes (~21 kJ/mol), developing adsorbents with high CO_2 selectivity, robust structural stability, and low cost is of critical urgency. Small molecule adsorbents have emerged as promising candidates for CO_2 capture owing to their rapid adsorption kinetics, low desorption temperatures (<120 °C), and affordable synthetic costs. This review first outlines the major categories of direct air capture (DAC) adsorbents—including alkali/alkaline earth-based, framework, and amine-based sorbents—and comparatively evaluates their key performance metrics. It then focuses on recent advances in small molecule adsorbents for DAC, with particular emphasis on the design principles and application scenarios of supramolecular host architectures with diverse topologies (linear, multi-arm, cyclic, and cage-shaped). These adsorbents typically incorporate hydrogen-bond donor motifs (e.g., amino, ureido, thiourea, and guanidino groups) that immobilize CO_2 via non-covalent interactions with HCO_3^-/CO_2 species. The practical deployment of small molecule DAC adsorbents in industrial settings is further summarized. Finally, existing technical bottlenecks are identified, and future research directions for next-generation adsorbent design are proposed.

Keywords: *small molecule adsorbents; CO_2 capture; anion coordination; hydrogen bonding; organic amines*

Received on 10 Apr 2022, Accepted on 15 June 2022, Published on 08 July 2022

1 Introduction

Since the onset of the Industrial Revolution, anthropogenic CO_2 emissions have risen continuously, driving cascading environmental crises including global warming, ocean acidification, and biodiversity loss, which pose direct threats to ecological security and human well-being. There is thus an urgent imperative to develop efficient CO_2 capture technologies to curb emission growth and reverse the trend of climate change. Direct air capture (DAC) — the extraction of CO_2 directly from ambient air — is an emerging carbon mitigation technology with vast deployment potential. Conventional CO_2 capture systems are plagued by persistent limitations, including low adsorbent capacity, high capital expenditure, and poor cycling stability [1 – 4]. Consequently, the development of adsorbents that combine high capture efficiency with low-temperature regenerability has become a focal point of current research. Widely used DAC adsorbent classes include alkali/alkaline earth-based sorbents [5], porous framework materials [6], and organic amine sorbents [7]; however, their practical implementation remains constrained by inadequate cycling durability and prohibitive costs. Unlike covalent-interaction-driven CO_2 adsorption pathways, non-covalent mechanisms (e.g., electrostatic attraction, hydrogen bonding) can substantially reduce the thermal energy demand for adsorbent regeneration. Small molecule adsorbents offer distinct advantages including structural diversity and facile functional tunability; rational structure – property relationship studies enable the design of adsorbents that simultaneously achieve high capacity and low regeneration energy consumption.

This review provides a concise overview of mainstream DAC adsorbent categories and their practical deployment status, followed by a critical evaluation of their respective strengths and weaknesses. It places particular emphasis on non-covalent CO_2 adsorption mechanisms and recent progress in small molecule adsorbent development, outlines the current industrial landscape of DAC technologies (process design, cost structure, site selection criteria), and offers forward-looking perspectives on the evolution of small molecule adsorbent systems.

2 Adsorbent Taxonomy

Current DAC technologies primarily employ three classes of adsorbents: alkali/alkaline earth-based sorbents (e.g., NaOH, KOH, $Ca(OH)_2$), porous framework sorbents [6], and amine-functionalized sorbents [7].

2.1 Alkali/Alkaline Earth-Based Sorbents

Alkali-based sorbents are well-suited for large-scale deployment, with demonstrated annual capture capacities of up to 9800 t CO_2 under full-load operation. Their CO_2 capture chemistry proceeds via the following reactions [8]:

Carbonation: $M_2CO_3 + CO_2 + H_2O \rightarrow 2MHCO_3$ (1)

Regeneration: $2MHCO_3 \rightarrow M_2CO_3 + CO_2 + H_2O$ (2)

where M denotes alkali metals. Carbonation typically occurs at 333–383 K, while sorbent regeneration requires temperatures of 373–473 K. The theoretical CO_2 uptake of bulk Na_2CO_3 reaches 6.4 mmol/g [9]. The carbonation of alkali sorbents (a gas–solid reaction) is governed by three sequential steps: gas-phase diffusion to the solid surface, intraparticle adsorption, and intrinsic chemical reaction. To enhance dispersion and kinetics, alkali active phases are commonly supported on high-surface-area, mesoporous carriers (e.g., carbon, ZrO_2, SiO_2, Al_2O_3) in fixed-bed or fluidized-bed reactor configurations.

PACCIANI et al. [10] reported a Li_2SiO_4-based alkali sorbent with a saturation capacity of 5.4 mmol/g and a desorption temperature of 547 K; however, the material suffered from 23%–25% capacity decay within the first 10 adsorption–desorption cycles before stabilizing. SEGGIANI et al. [11] demonstrated that Li_2SiO_4/Na_2CO_3 composites exhibited markedly improved cycling stability: a 30 wt% Na_2CO_3 loading retained 100% of the initial capacity over 25 cycles. RADA et al. [12] developed a Li_8SiO_6 sorbent with a high uptake of 11.8 mmol/g across a broad temperature window. GAMMIE et al. [13] synthesized a Na_2ZrO_3 sorbent that achieved a maximum capacity of 4.32 mmol/g at a heating rate of 1 °C/min under pure CO_2 flow. While alkali/alkaline earth sorbents deliver high gravimetric capacities, practical deployment must address equipment corrosion risks and long-term cycling durability. Key performance metrics of representative alkali-based DAC sorbents are summarized in Table 1.

Table 1 Key performance metrics of alkali-based sorbents for direct air CO_2 capture

Adsorbent	CO_2 uptake/(mmol·g^{-1})	Regeneration temperature/K	Ref.
Li_2CO_3	—	373–473	[9]
Na_2CO_3	6.4	373–473	[9]
Li_2SiO_4	5.4	547	[10]
Li_8SiO_6	11.8	—	[12]

Adsorbent	CO_2 uptake/(mmol·g^{-1})	Regeneration temperature/K	Ref.
Na_2ZrO_3	4.32	—	[13]

Note: "—" indicates data not reported in the original reference; same hereinafter.

2.2 Framework Sorbents

Porous framework materials feature tailorable topologies, ultrahigh surface areas, and tunable pore chemistries, enabled by modular ligand design and metal node selection [14]. CO_2 adsorption in these materials arises from a combination of physisorption within pores and chemisorption via electrostatic interactions at active sites. However, their performance is highly sensitive to pore structure stability: repeated adsorption–desorption cycles often lead to pore collapse. Furthermore, in humid flue gas or ambient air, competitive adsorption between H_2O and CO_2 reduces selectivity, while pore-confined water elevates desorption temperatures. Surface hydrophobization or novel framework design is therefore required to maintain structural integrity under moist conditions [6]. Common performance-enhancement strategies include doping with redox-active metal nodes (Mg, Zn, Co, Ni) and post-synthetic amine functionalization. Representative framework sorbents for DAC are listed in Table 2.

Table 2 Key performance metrics of framework sorbents for direct air CO_2 capture

Adsorbent	CO_2 uptake/(mmol·g^{-1})	Regeneration enthalpy/(kJ·mol^{-1})	Regeneration temperature/°C	Ref.
HKUST-1@SWCNT	8.23	—	—	[15]
ZIF-8@beech	2.14	—	—	[16]
RHA@MIL-101(Cr)	0.43	20	—	[17]
COF-999	2.05	53	60	[18]
CuBTC@GA	3.26	—	—	[19]
ZnH-MFU-4	3.12	130	300	[20]
$Ni_3(HTIP)_2$	1.25	72.4	Potential-controlled	[21]
MOF-Zn-OH	2.2	71	100	[22]
MOF-Ni-OH	2.7	84	100	[23]

Note: HKUST-1@SWCNT = single-walled carbon nanotube-supported copper-based metal–organic framework; ZIF-8@beech = in situ grown zeolitic imidazolate framework on wood substrate; RHA@MIL-101(Cr) = rice husk ash-doped chromium-based MOF; COF-999 = olefin-linked covalent organic framework; CuBTC@GA = graphene aerogel-composited copper tricarboxylate framework; ZnH-MFU-4 = zinc hydride-functionalized porous MOF; $Ni_3(HTIP)_2$ = conductive nickel-based framework; MOF-Zn-OH/Ni-OH = hydroxyl-decorated zinc/nickel MOFs.

2.3 Amine-Based Sorbents

Amine scrubbing is a mature, widely deployed CO_2 capture technology, predominantly used for flue gas treatment in power and cement plants [24]. Common amine sorbents include monoethanolamine (MEA), diethanolamine (DEA), N-methyldiethanolamine (MDEA), and 2-amino-2-methyl-1-propanol (AMP). In aqueous or aprotic solvents (e.g., DMSO, DMF), amines react with CO_2 to form carbamic acid or bicarbonates [25], which can be thermally decomposed to release pure CO_2 for sorbent recycling. The underlying reaction pathways are as follows [11]:

$$2\,RNH_2 + CO_2 \rightleftharpoons RNHCO_2^- + RNH_3^+ \quad (3)$$

$$R_1R_2R_3N + CO_2 + H_2O \rightleftharpoons R_1R_2R_3NH^+ + HCO_3^- \quad (4)$$

Amines are classified into primary, secondary, and tertiary species based on the number of alkyl substituents on the nitrogen atom. Primary and secondary amines react rapidly with CO_2 to form carbamic acid in anhydrous media [Eq. (3)], whereas tertiary amines exhibit slower direct reactivity due to steric hindrance and require water to facilitate bicarbonate formation [Eq. (4)]. Notably, the nitrogen center in tertiary amines acts as a proton shuttle, lowering the activation barrier for carbamate decomposition and thereby reducing regeneration energy demand.

Despite widespread industrial adoption, conventional amine systems face trade-offs between high capacity and low regeneration energy, alongside substantial heat duty penalties during desorption [26]. To resolve this, LYU et al. [27] formulated blended amine solvents combining fast-reacting primary/secondary amines with proton-accepting tertiary amines: the former rapidly capture CO_2 to form carbamates, while the latter accept protons to alter the decomposition pathway, as illustrated in Fig. 1.

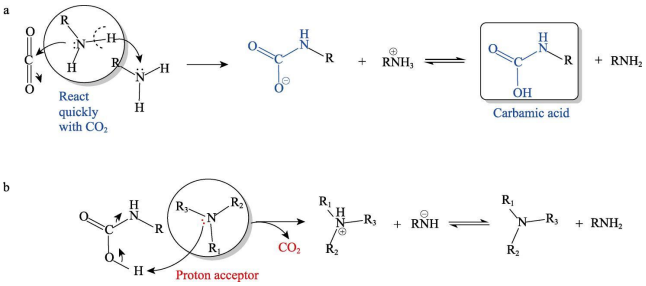

Figure 1 Schematic of CO_2 absorption mechanism in physically mixed amine systems [27]

Practical deployment must also account for solubility mismatches between amine components and the tendency of long-chain aliphatic amines to form viscous gels post-adsorption, which can foul process equipment.

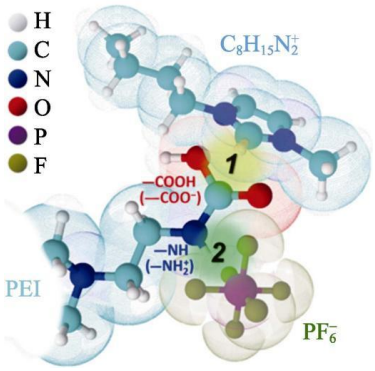

Figure 2 Interaction mechanism between ionic liquids and carbamic acid [28]

To further reduce regeneration energy, LIU et al. [28] replaced water with ionic liquids (ILs); electrostatic interactions between IL ions and carbamate zwitterions weaken the C–N bond, lowering the desorption barrier (Fig. 2). WEISSHAR et al. [29] developed a [$C_8H_{15}N_2PF_6$-PEI] system where IL incorporation reduced the regeneration temperature by ≥30 °C, enabling sorbent recovery at 50 °C.

To enhance CO_2 binding affinity, LI et al. [30] designed a cage-shaped “superfan” adsorbent that outperforms linear aliphatic amines for CO_2 capture from dilute streams (flue gas, exhaled air, indoor air) (Fig. 3). Mechanical stirring enabled room-temperature CO_2 release and concentration, increasing the CO_2 volume fraction in exhaled breath from 6% to 83%. The mechanism likely involves formation of a stable six-membered ring transition state between the superfan and CO_2. This represents the first liquid-phase DAC system capable of low-energy CO_2 release via mechanical input.

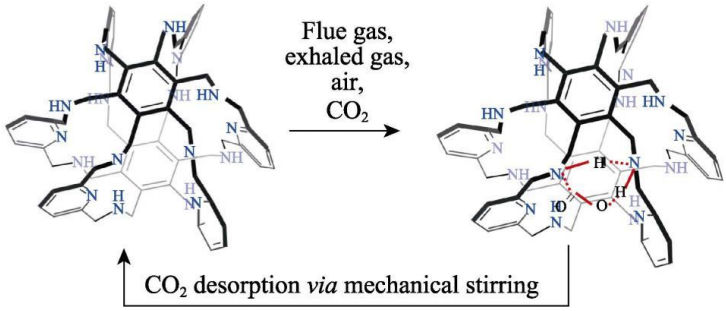

Figure 3 Superfan-mediated CO_2 adsorption via six-membered ring formation, with room-temperature release enabled by mechanical stirring [30]

Small molecule adsorbents combine high reactivity, structural robustness, and low regeneration energy demand, positioning them as promising next-generation DAC platforms [31]. While covalent CO_2 capture by amines is well-documented [32,33], this review focuses on non-covalent small molecule adsorbents that bind HCO_3^-/CO_3^{2-} via hydrogen bonding or electrostatic interactions.

3 Non-Covalent Interaction-Driven CO_2 Adsorption

Non-covalent CO_2 capture mechanisms—particularly hydrogen bonding—substantially reduce the thermal energy required for sorbent regeneration. Typical hydrogen bond donor motifs include amino, ureido, thiourea, and guanidino groups. The process generally involves adding tetrabutylammonium fluoride (TBAF) to elevate solution OH^- concentration, which converts atmospheric CO_2 to HCO_3^-/CO_3^{2-}; the adsorbent (L) then binds these anions via non-covalent interactions:

$$F^- + H_2O \rightarrow HF + OH^- \quad (5)$$

$$OH^- + CO_2 \rightarrow HCO_3^- \quad (6)$$

$$L + HCO_3^- \rightarrow L{\cdot}HCO_3^- \quad (7)$$

This section categorizes non-covalent small molecule adsorbents by their hydrogen bond donor architecture and summarizes recent advances.

3.1 Amino-Functionalized Small Molecule Adsorbents

GUNNLAUGSSON et al. [34] developed a naphthalimide-based adsorbent 1: in the presence of F^-, deprotonation of -NHR induced a color shift from green to purple. Isolation of the [(1)·(F^-)] complex revealed that elevated solution alkalinity enabled interfacial CO_2 capture to form HCO_3^-, which bound to 1 in a 2:2 stoichiometry via hydrogen bonding. A unique anti-electrostatic hydrogen bond was observed between the two encapsulated HCO_3^- anions (Fig. 4).

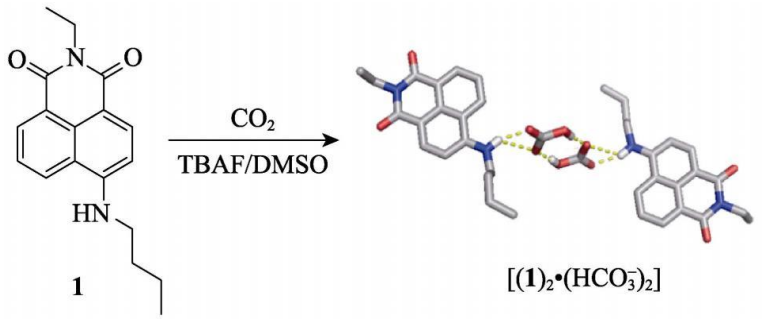

Figure 4 CO_2 capture mechanism of naphthalimide-based adsorbent 1 [34]

3.2 Oligourea Small Molecule Adsorbents

3.2.1 Linear Oligourea Architectures

BOIOCCHI et al. [35] designed monourea 2: a 1:1 molar ratio with TBAF yielded the $[(2)\cdot(F^-)]$ complex, while a 1:2 ratio produced the $[(2)_2\cdot(HCO_3^-)_2]$ adduct. Excess F^- elevated OH^- levels [Eq. (5)], driving CO_2-to-HCO_3^- conversion and subsequent binding (Fig. 5). Each HCO_3^- formed a dimer via O–H···O hydrogen bonds, stabilized by two N–H···O and three weak C–H···O interactions with the ligand. CHUTIA et al. [36] later reported a para-iodophenyl monourea 3 that formed an analogous $[(3)_2\cdot(HCO_3^-)_2]$ complex, where halogen bonding supplemented hydrogen bonding for dimer stabilization.

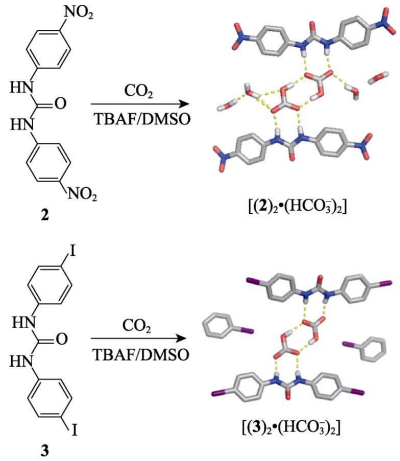

Figure 5 CO_2 capture mechanism of oligoureas 2 and 3 [35,36]

MANNA et al. [37] synthesized a series of meta/para-substituted diaryl diureas (4–7) with electron-withdrawing $-CF_3$ or -Cl termini. In the presence of F^-/OH^-, atmospheric CO_2 was converted to HCO_3^-/CO_3^{2-} and encapsulated via hydrogen bonding (Fig. 6). For example, trifluoromethylphenyl diurea 4 formed a 2:1 $[(4)_2\cdot(CO_3^{2-})]$ complex, with CO_3^{2-} stabilized by N–H···O and C–H···O interactions. Meta-phenylene-linked diurea 5 yielded a 2:2 $[(5)_2\cdot(HCO_3^-)_2]$ assembly, where HCO_3^- dimers were further stabilized by inter-anion O–H···O bonds [38].

In TBAOH-containing DMF/DMSO mixtures, diureas 6 and 7 [39,40] formed $[(6)_4\cdot(H_2O)\cdot(CO_3^{2-})_2]$ and $[(7)_2\cdot(HCO_3^-)_2]$ complexes, respectively (Fig. 7). Four molecules of 6 assembled into a columnar structure stabilized by 16 N–H···O and 7 C–H···O bonds; unlike 2, the diurea backbone of 7 enabled infinite framework formation.

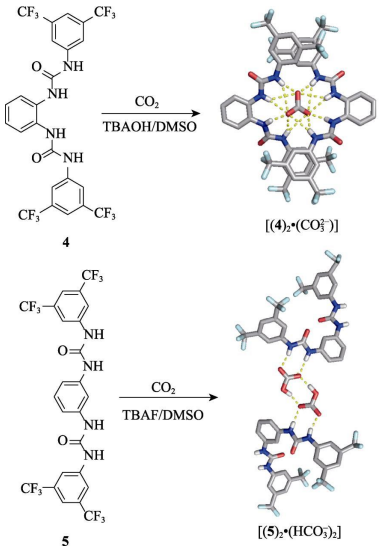

Figure 6 CO_2 capture mechanism of oligoureas 4 and 5 [37,38]

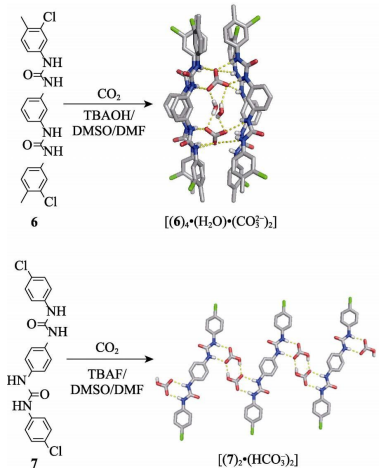

Figure 7 CO_2 capture mechanism of oligoureas 6 and 7 [39,40]

3.2.2 Multi-Arm Oligourea Architectures

Multi-arm oligoureas offer enhanced preorganization and three-dimensional encapsulation compared to linear analogues. Nitrobenzene-terminated tripodal triurea 8 [41] and cyanobenzene-terminated 9 [42] formed 2:1 sandwich complexes [$(8)_2 \cdot (CO_3^{2-})$] and [$(9)_2 \cdot (CO_3^{2-})$] in TBAOH, with quantitative sorbent regeneration achievable in 1:4 (v/v) methanol–water (Fig. 8).

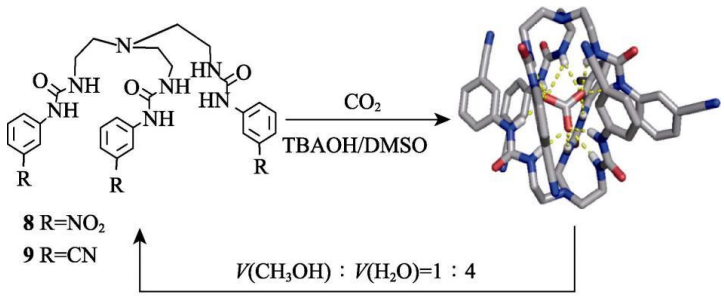

Figure 8 CO_2 capture mechanism of oligoureas 8 and 9 [41,42]

RAVIKUMAR et al. [43] developed a pentafluorophenyl-terminated triurea 10 that formed the $[(10)_2 \cdot (CO_3^{2-})]$ complex in TBAOH (Fig. 9). Single-crystal analysis showed six urea N–H groups pointing inward to encapsulate CO_3^{2-} via hydrogen bonding. ^{13}C NMR confirmed encapsulation: the bicarbonate signal shifted from δ 159 to 170. Treatment with 1:4 methanol–water fully regenerated 10, with >99% purity verified by spectroscopy and diffraction.

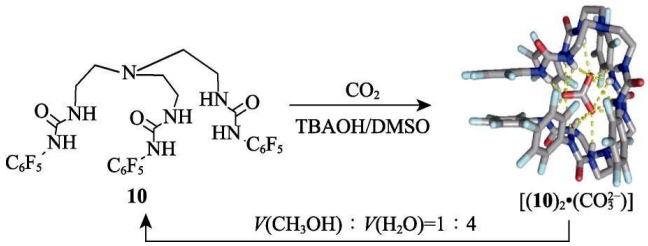

Figure 9 CO_2 capture mechanism of oligourea 10 [43]

PRAMANIK et al. [44] designed a tripodal hexaurea 11 with higher preorganization and more binding sites (Fig. 10). NMR titration gave a HCO_3^- binding constant of 1780 mol/L in DMSO-d_6. Crystal structures revealed a 1:1 $[(11)\cdot(CO_3^{2-})]$ complex, with 12 N–H···O bonds locking CO_3^{2-} in the cavity. The chelate effect endows this architecture with exceptional anion affinity.

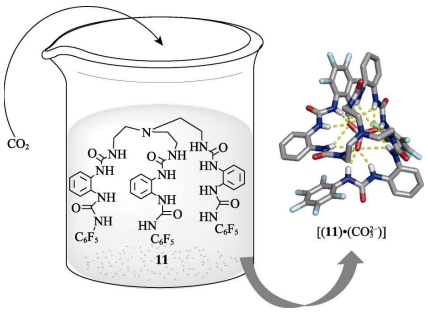

Figure 10 CO_2 capture mechanism of oligourea 11 [44]

MANNA et al. [45] and KAYAL et al. [46] independently reported tripodal oligothiourea adsorbents 12 and 13, which formed $[(12)_2 \cdot (CO_3^{2-})]$ and $[(13)_2 \cdot (CO_3^{2-})]$ complexes under alkaline conditions (Fig. 11), with CO_2 release again triggered by 1:4 methanol–water.

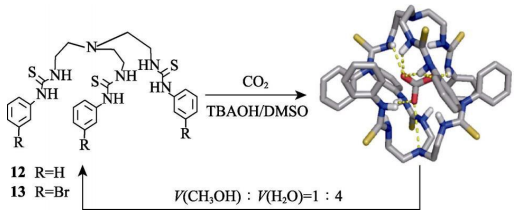

Figure 11 CO_2 capture mechanism of oligothioureas 12 and 13 [45,46]

3.2.3 Cyclic Oligourea Architectures

BROOKS et al. [47] synthesized a macrocyclic urea 14; excess TBAF in DMSO yielded co-crystals of F^- and CO_3^{2-} (Fig. 12). CO_3^{2-} was encapsulated in the macrocycle cavity via urea hydrogen bonds, while F^- was stabilized outside the cavity by O–H···F interactions with four lattice water molecules, which also formed hydrogen bonds with the macrocycle.

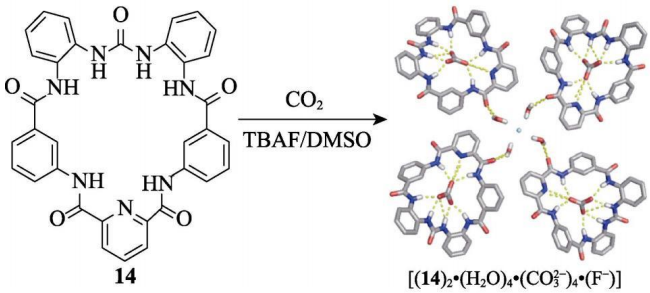

Figure 12 CO_2 capture mechanism of cyclic oligourea 14 [47]

3.3 Guanidine-Based Adsorbents

Guanidines bind oxygen-containing anions via hydrogen bonding, enabling separation via crystallization. Electron-withdrawing substitution enhances guanidine acidity, strengthening anion binding and crystallization efficiency.

SEIPP et al. [48] designed a 2,6-pyridyl bisimidoguanidine 15 that formed a crystalline [(15)·H_2 (CO_3)(H_2 O)$_4$] complex (Ksp = 1.0×10^{-8}) upon CO_2 exposure (Fig. 13). Heating to 80–120 °C released CO_2 and regenerated the sorbent. The non-covalent binding mechanism reduces regeneration energy relative to covalent amine systems. WILLIAMS et al. [49] reported a similar bisimidoguanidine 16 that crystallized as [(16)·H_2 (HCO_3^-)$_2$ (H_2 O)$_2$] and retained full capacity over 10 cycles. Its regeneration energy (151.5 kJ/mol) is 24% lower than that of industrial MEA, representing one of the most efficient small molecule DAC systems to date.

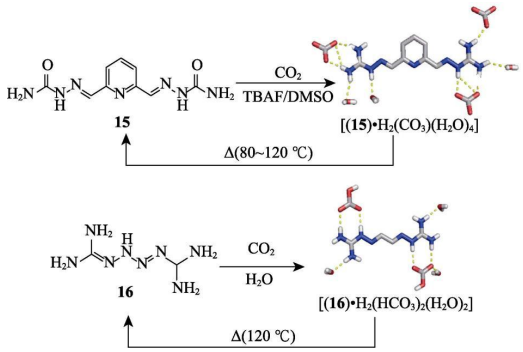

Figure 13 Atmospheric CO_2 capture via crystallization of guanidine adsorbents 15 and 16 [48,49]

3.4 Pyran-Based Photoswitchable Adsorbents

ALFARAIDI et al. [50] developed a pyran-based adsorbent 17 that reversibly switches between closed (SP) and open (MC) isomers under light irradiation, enabling CO_2 capture and release via electrostatic interactions (Fig. 14). Such photoswitchable systems represent a promising direction for low-energy DAC, though the thermodynamics and photochemical mechanisms require further optimization.

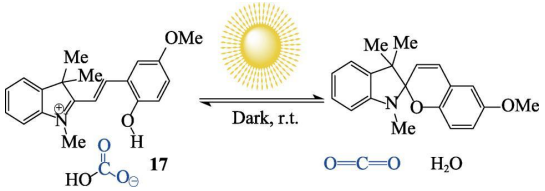

Figure 14 Photo-triggered CO_2 capture and release via pyran isomerism [50]

3.5 Metal Self-Assembled Adsorbents

LI et al. [51] constructed flexible tetraazacyclododecane-based assemblies [(Me_4 enPd)$_2$ (ML) , n=2/3, M = Zn, Co, Ni, Cu, Pd, Ag]. The Zn analogue (18-Zn) exhibited exceptional acid/base stability (stable at pH 1–12) and served as an efficient CO_2 fixator (Fig. 15). Injecting CO_2 into a 18-Zn/NaOH DMSO-d_6 /D_2O solution produced a ^{13}C NMR signal at δ 160, confirming carbonate formation. DFT calculations revealed a two-step mechanism: Zn–OH nucleophilic attack on CO_2 (rate-determining step) followed by deprotonation to CO_3^{2-}, with a binding energy of 1349 kJ/mol.

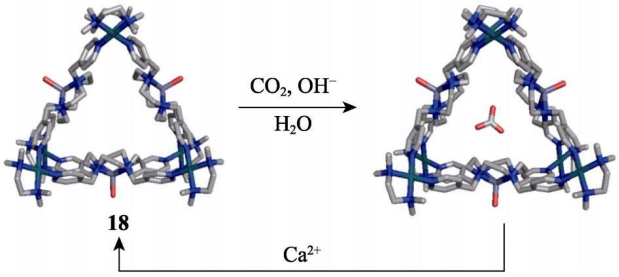

Figure 15 CO_2-to-carbonate conversion by 18-Zn self-assemblies [51]

MURASE et al. [52] demonstrated that trinuclear zinc complex Zn_3 L (19) captured CO_2 in EMIM-Tf_2N ionic liquid to form [Zn_3 L-CO_3]$^{4+}$, with ^{13}C NMR verifying carbonate formation (Fig. 16). Electrochemical reduction triggered CO_2 release, offering a non-thermal regeneration pathway. EMAD et al. [53] synthesized Ni/Co/Cu sulfamethoxazole complexes 20, where metal Lewis acidity enhanced CO_2 binding; the Co complex delivered the highest uptake (26.1 cm^3/g), attributed to its larger pore volume (0.018 cm^3/g) and surface roughness. Long-term cycling stability remains to be evaluated.

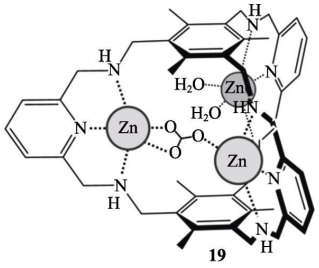

Figure 16 Structure of $[Zn_3L\text{-}CO_3]^{4+}$ complexes [52]

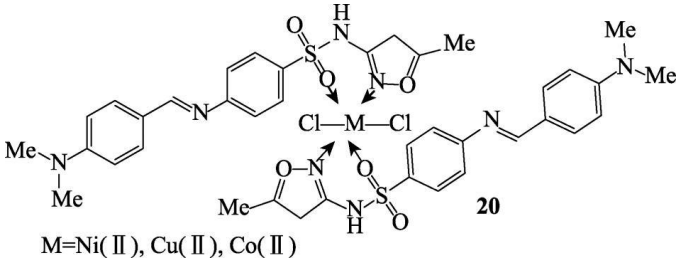

Figure 17 Structure of sulfamethoxazole-metal complexes [53]

Key performance metrics of non-covalent DAC adsorbents are summarized in Table 3.

Table 3 Key performance metrics of non-covalent small molecule DAC adsorbents

Adsorbent	Binding mode	Post-adsorption species	Adsorption condition	Regeneration method	Ref.
1	H-bonding	$[(1)_2 \cdot (HCO_3^-)_2]$	TBAF/DMSO	—	[34]
2	H-bonding	$[(2)_2 \cdot (HCO_3^-)_2]$	TBAF/DMSO	—	[35]
3	H-bonding	$[(3)_2 \cdot (HCO_3^-)_2]$	TBAF/DMSO	—	[36]
4	H-bonding	$[(4)_2 \cdot (CO_3^{2-})]$	TBAOH/DMSO	—	[37]
5	H-bonding	$[(5)_2 \cdot (HCO_3^-)_2]$	TBAF/DMSO	—	[38]
6	H-bonding	$[(6)_4 \cdot (H_2O) \cdot (CO_3^{2-})_2]$	TBAOH/DMSO/DMF	—	[39]
7	H-bonding	$[(7)_2 \cdot (HCO_3^-)_2]$	TBAOH/DMSO/DMF	—	[40]
8	H-bonding	$[(8)_2 \cdot (CO_3^{2-})]$	TBAOH/DMSO	—	[41]
9	H-bonding	$[(9)_2 \cdot (CO_3^{2-})]$	TBAOH/DMSO	—	[42]
10	H-bonding	$[(10)_2 \cdot (CO_3^{2-})]$	TBAOH/DMSO	1:4 MeOH/H_2O	[43]
11	H-bonding	$[(11) \cdot (CO_3^{2-})]$	TBAF/DMSO	1:4 MeOH/H_2O	[44]
12	H-bonding	$[(12)_2 \cdot (CO_3^{2-})]$	TBAOH/DMSO	1:4 MeOH/H_2O	[45]
13	H-bonding	$[(13)_2 \cdot (CO_3^{2-})]$	TBAOH/DMSO	1:4 MeOH/H_2O	[46]
14	H-bonding	$[(14)_2 \cdot (H_2O)_4 \cdot (CO_3^{2-})_4 \cdot (F^-)]$	TBAF/DMSO	—	[47]
15	Electrostatic	$[(15) \cdot H_2(CO_3)(H_2O)_4]$	H_2O	80–120 °C	[48]
16	Electrostatic	$[(16) \cdot H_2(HCO_3^-)_2(H_2O)_2]$	H_2O	120 °C	[49]
17	Electrostatic	$[(17) \cdot (HCO_3^-)]$	H_2O	Light irradiation	[50]
18	Metal coordination	$[Zn^{2+}(18) \cdot (CO_3^{2-})]$	H_2O/NaOH	Ca^{2+} precipitation	[51]
19	Metal	$[Zn^{2+}{}_3(19) \cdot (CO_3^{2-})(CH_3CN)(H_2O)_4]$	CH_3OH/CH_3CN	Electrolysis	[52]

Adsorbent	Binding mode	Post-adsorption species	Adsorption condition	Regeneration method	Ref.
	coordination				
20	Metal coordination	[Co^{2+} (20)·(CO_3^{2-})]	—	—	[53]

4 Industrial Deployment of DAC Technology

4.1 Practical Application Scenarios

DAC technology originated in the 1930s for spacecraft life support, removing CO_2 from cabin air [54]. The low atmospheric CO_2 concentration (~415 ppm) favors strongly binding chemisorbents, which are extensively studied in academic literature. Unlike aqueous systems, solid sorbents require only low-temperature regeneration (80–100 °C), enabling integration with industrial waste heat from power plants, steel mills, or glass factories [55]. DEREVSCHIKOV et al. [55] proposed converting captured CO_2 to methane fuel via composite solid sorbents. GOLDBERG et al. [56] combined DAC with offshore wind power and sub-seabed CO_2 storage. Emerging approaches include charged-sorbent DAC [57] and nanofiltration-based separation [58], with projected costs as low as US$13.7/t CO_2. While guanidine-based crystalline capture shows early promise [48], pilot-scale validation is required for technology readiness assessment.

4.2 Current Commercial Landscape

Commercial DAC technologies fall into two categories: high-temperature liquid sorbent systems (HTLS-DAC) and low-temperature solid sorbent systems (LTSS-DAC) [58]. Leading global DAC developers and their performance metrics are summarized in Table 4. Climeworks (Switzerland, 2007) and Global Thermostat (USA, 2010) project baseline costs of ~US$600/t CO_2; Global Thermostat supplies captured CO_2 to Coca-Cola for beverage carbonation. Infinitree (USA) integrates enrichment processes from Kilimanjaro and Global Research Technologies. Water consumption is a key site-selection constraint: HTLS-DAC loses 0–50 t water per ton of CO_2 captured, limiting deployment to humid regions. In contrast, LTSS-DAC recovers water as a by-product (0.8–2 t H_2O/t CO_2 for Climeworks), giving it a distinct advantage for arid-zone deployment [59].

Table 4 Commercialized DAC technologies

Company	Country	DAC type	Adsorbent	Projected cost/(USD·t^{-1} CO_2)	Ref.
Carbon Engineering	Canada	HTLS	KOH aqueous solution	158	[5]
Antecy	Netherlands	LTSS	K_2CO_3	177	[57]
Global Thermostat	USA	LTSS	Amine-grafted porous silica	—	[60]
Hydrocell	Finland	LTSS	Amine-functionalized polystyrene	—	[61]
Kieth	Canada	HTLS	KOH aqueous solution	200	[62]

5 Conclusions and Future Outlook

This review summarizes recent advances in small molecule adsorbents for DAC, with a focus on adsorption mechanisms, performance benchmarking, and industrial deployment status. While substantial progress has been made in fundamental research, several critical challenges remain:

(1) Practical applicability: Few existing materials balance all key DAC metrics (capacity, selectivity, kinetics, cycling stability). Inorganic sorbents (e.g., alumina, zeolites) suffer from limited tunability, while mesoporous silica—especially amine-functionalized variants—offers a promising platform for tailored design. Maintaining framework stability under humid, variable-temperature conditions is essential for flue gas applications. Future work should prioritize scalable, low-cost synthesis routes compatible with industrial deployment.

(2) Product valorization: Beyond capture, downstream CO_2 utilization is critical for economic viability. Current applications are limited to beverage carbonation; future efforts should target conversion to value-added chemicals (methanol, methane, ethylene) to close the carbon cycle.

(3) Long-term durability: Most studies report short-term cycling data; systematic evaluation of adsorbent aging, impurity tolerance, and multi-year stability is required for commercial feasibility assessment.

(4) Structure – property relationships: Quantitative understanding of how molecular topology, binding site density, and non-covalent interaction strength govern DAC performance is lacking. Combined experimental–computational studies are needed to guide rational adsorbent design. Process engineering optimization (reactor configuration, heat integration) is equally critical for overall system efficiency.

Small molecule adsorbents represent a rapidly evolving frontier in DAC technology. Future breakthroughs will hinge on balancing economic feasibility, low regeneration energy, and circular carbon utilization, enabled by integrated insights into molecular design, materials science, and process engineering.

References

[1] Custelcean R. Direct air capture of CO_2 using solvents. Annual Review of Chemical and Biomolecular Engineering, 2022, 13(1): 217–234.
[2] Custelcean R, Garrabant K, Agulio P, et al. Direct air capture of CO_2 with aqueous peptides and crystalline guanidines. Cell Reports Physical Science, 2021, 2(4): 100385.
[3] Renforth P, Wilcox J. The role of negative emission technologies in addressing our climate goals. Frontiers in Climate, 2020, 2: 1–3.
[4] Azarabadi H, Lackner K. A sorbent-focused techno-economic analysis of direct air capture. Applied Energy, 2019, 250: 959–975.
[5] Keith D, Holmes G, Angelo D, et al. A process for capturing CO_2 from the atmosphere. Joule, 2018, 2(8): 1573–1594.
[6] Gebremariam S, Dumee L, Liewellyn P, et al. Metal-organic framework hybrid adsorbents for carbon capture. Journal of Environmental Chemical Engineering, 2021, 11(2): 109291.
[7] Zhang Y, Gao Y S, Pfeiffer H, et al. Recent advances in lithium containing ceramic based sorbents for high-temperature CO_2 capture. Journal of Materials Chemistry A, 2019, 7(14): 7962–8005.
[8] Zhao R L, Ma W T, Xu X, et al. Research progress of carbon capture chemical absorbents. Fine Chemicals, 2021, 40(1): 1–9.
[9] Tong Y C, Chen S Z, Huang X, et al. CO_2 capture by Li_4SiO_4 sorbent: From fundamentals to applications. Separation and Purification Technology, 2022, 301: 121977.
[10] Pacciani R, Torres J, Vefa L F, et al. Influence of the concentration of CO_2 and SO_2 on the absorption of CO_2 by a lithium orthosilicate-based absorbent. Environmental Science & Technology, 2011, 45(16): 7083 – 7088.
[11] Seggiani M, Puccini M, Vitolo S. Alkali promoted lithium orthosilicate for CO_2 capture at high temperature and low concentration. International Journal of Greenhouse Gas Control, 2013, 17: 25–31.
[12] Rada E, Moreno M S. Synthesis of high purity Li_8SiO_6 using a citric acid-assisted route. Ceramics

International, 2022, 48(8): 11273–11277.
[13] Gammie C, Hesse F, Kennedy B, et al. Encoding CO_2 adsorption in sodium zirconate by neutron diffraction. Molecules, 2022, 29(16): 3798.
[14] Liu G P, Cadiau A, Liu Y, et al. Enabling fluorinated MOF-based membranes for simultaneous removal of H_2S and CO_2 from natural gas. Angewandte Chemie International Edition, 2018, 130(45): 15027–15032.
[15] Cortes J, Celis V, Beltran H I, et al. Synthesis and characterization of an SWCNT@HKUST-1 composite: Enhancing the CO_2 adsorption properties of HKUST-1. ACS Omega, 2019, 4(3): 5275–5282.
[16] Tu K, Puertolas B, Adobes M, et al. Green synthesis of hierarchical metal-organic framework/wood functional composites with superior mechanical properties. Advanced Science, 2020, 7(7): 1902897.
[17] Panada D, Saini C, Kumar E A, et al. In-situ casting of rice husk ash in metal organic frameworks induces enhanced CO_2 capture performance. Scientific Reports, 2020, 10(1): 20219.
[18] Zhou Z H, Ma T, Zhang H, et al. Carbon dioxide capture from open air using covalent organic frameworks. Nature, 2022, 635(8037): 96–101.
[19] Ren W, Wei Z Z, Xia X X, et al. CO_2 adsorption performance of CuBTC/graphene aerogel composites. Journal of Nanoparticle Research, 2020, 22(7): 1–9.
[20] Rohde R C, Carsch K M, Dods M N, et al. High-temperature carbon dioxide capture in a porous material with terminal zinc hydride sites. Science, 2022, 386(6723): 814–819.
[21] Liu J X, Yang M Y, Zhou X Y, et al. Solid-state electrochemical carbon dioxide capture by conductive metal-organic framework incorporating nickel bis(diimine) units. Journal of the American Chemical Society, 2022, 146(48): 33093–33103.
[22] Bien C E, Chen K K, Chien S C, et al. Bioinspired metal-organic framework for trace CO_2 capture. Journal of the American Chemical Society, 2018, 140(40): 12662–12666.
[23] Bien C E, Liu Q, Wade C R. Assessing the role of metal identity on CO_2 adsorption in MOFs containing M-OH functional groups. Chemistry of Materials, 2019, 32(1): 489–497.
[24] Xu Y H, Xiao B H, Feng Y Y, et al. Research progress of carbon dioxide capture materials. Fine Chemicals, 2021, 38(8): 1513–1521.
[25] Hamp E, Rudkevich D. Exploring reversible reactions between CO_2 and amines. Tetrahedron, 2003, 59(48): 9619–9625.
[26] Wen H, Han W, Che X, et al. Progress in post combustion carbon dioxide capture technology and application. Fine Chemicals, 2022, 39(8): 1584–1595.
[27] Lyu B H, Yang K X, Zhou X B, et al. 2-Amino-2-methyl-1-propanol based non-aqueous absorbent for energy-efficient and non-corrosive carbon dioxide capture. Applied Energy, 2020, 264: 114703.
[28] Liu F, Shen Y, Shen L, et al. Novel amino-functionalized ionic liquid/organic solvent with low viscosity for CO_2 capture. Environmental Science & Technology, 2020, 54(6): 3520–3529.
[29] Weisshar F, Gau A, Hack J, et al. Toward carbon dioxide capture from the atmosphere: Lowering the regeneration temperature of polyethylenimine-based adsorbents by ionic liquid. Energy & Fuels, 2021, 35(10): 9059–9062.
[30] Li A M, Liu Y C, He Q, et al. CO_2 capture in liquid phase and room-temperature release and concentration using mechanical power. CCS Chemistry, 2022, 6: 2882–2894.
[31] Manna U, Das G. An overview of CO_2/HCO_3^- binding by aerial CO_2 fixation within the self-assemblies of hydrogen-bond donor scaffolds. CrystEngComm, 2021, 23(3): 512–527.
[32] Dellamico D, Calderazzo F, Labella L, et al. Converting carbon dioxide into carbamato derivatives. Chemical Reviews, 2004, 103(10): 3857–3898.
[33] Soo X Y D, Lee J J C, Wu W Y, et al. Advancements in CO_2 capture by adsorption and absorption: A comprehensive review. Journal of CO_2 Utilization, 2022, 81: 102727.
[34] Gunnlaugsson T, Kruger P, Jensen P, et al. Simple naphthalimide based anion sensors: Deprotonation induced colour changes and CO_2 fixation. Tetrahedron Letters, 2003, 44(49): 8909–8913.
[35] Boiocchi M, Boca L D, Gomez D, et al. Nature of urea-fluoride interaction: Incipient and definitive proton transfer. Journal of the American Chemical Society, 2004, 126(50): 16507–16514.
[36] Chutia R, Das G. Hydrogen and halogen bonding in a concerted act of anion recognition: F^--induced atmospheric CO_2 uptake by an iodophenyl functionalized simple urea receptor. Dalton Transactions, 2014, 43(41): 15628–15637.
[37] Manna U, Kayal S, Nayak B, et al. Systematic size mediated trapping of anions of varied dimensionality within a dimeric capsular assembly of a flexible neutral bis-urea platform. Dalton Transactions, 2017, 46(35): 11956–11969.

[38] Manna U, Das G. Anion binding consistency by influence of aromatic meta-disubstitution of a simple urea receptor: Regular entrapment of hydrated halide and oxyanion clusters. CrystEngComm, 2017, 19(37): 5622–5634.
[39] Manna U, Kayal S, Samanta S, et al. Fixation of atmospheric CO_2 as novel carbonate-H_2O-carbonate cluster and entrapment of double sulfate within a linear tetrameric barrel of a neutral bis-urea scaffold. Dalton Transactions, 2017, 46(31): 10374–10386.
[40] Manna U, Das G. Halo-phenyl based linear dipodal receptors for entrapment of anions/anionic associations within neutral non-cooperative self-assemblies. CrystEngComm, 2019, 21(1): 65–76.
[41] Dey S K, Chutia R, Das G. Oxyanion-encapsulated caged supramolecular frameworks of a tris(urea) receptor: Evidence of hydroxide and fluoride-ion-induced fixation of atmospheric CO_2 as a trapped CO_3^{2-} anion. Inorganic Chemistry, 2012, 51(3): 1727–1738.
[42] Dutta R, Chakraborty S, Ghosh P, et al. Aerial CO_2 trapped as CO_3^{2-} ions in a dimeric capsule that efficiently extracts chromate, sulfate, and thiosulfate from water by anion-exchange metathesis. European Journal of Inorganic Chemistry, 2014(25): 4134–4143.
[43] Ravikumar I, Ghosh P. Efficient fixation of atmospheric CO_2 as carbonate in a capsule of a neutral receptor and its release under mild conditions. Chemical Communications, 2010, 46(7): 1082–1084.
[44] Pramanik A, Khansari M, Powell D, et al. Absorption of atmospheric CO_2 as carbonate inside the molecular cavity of a new tripodal hexaurea receptor. Organic Letters, 2014, 16(2): 366–369.
[45] Manna U, Das G. Cyclic $(H_2O)_6$ confined hexameric host-guest assemblies and aerial CO_2 fixation by electron-rich neutral urea/thiourea scaffolds. CrystEngComm, 2018, 20(26): 3741–3754.
[46] Kayal S, Manna U, Das G. Fixation of atmospheric CO_2 and recognition of anions/hydrated anions: Differential binding mode in protonated vs. neutral tripodal urea/thiourea receptors. Inorganica Chimica Acta, 2019, 486: 576–581.
[47] Brooks S, Gale P, Light M. Anion-binding modes in a macrocyclic amidourea. Chemical Communications, 2006(41): 4344–4346.
[48] Seipp C, Williams N, Custelcean R, et al. CO_2 capture from ambient air by crystallization with a guanidine sorbent. Angewandte Chemie International Edition, 2017, 56(4): 1042–1045.
[49] Williams N, Seipp C, Custelcean R, et al. CO_2 capture via crystalline hydrogen-bonded bicarbonate dimers. Chem, 2019, 5(3): 719–730.
[50] Alfaraidi A M, Kudisch B, Thomas J, et al. Reversible CO_2 capture and on-demand release by an acidity-matched organic photoswitch. Journal of the American Chemical Society, 2021, 145(49): 26720–26727.
[51] Li S C, Liu C, Sun Q F, et al. Adaptive coordination assemblies based on a flexible tetraazacyclododecane ligand for promoting carbon dioxide fixation. Chemical Science, 2022, 13(31): 9016–9022.
[52] Murase M, Maegawa Y, Ohashi M, et al. Reversible CO_2 fixation and release by a trinuclear Zn(II) cryptate complex and operando analysis of the complex structure. ChemSusChem, 2021, 16(20): e202100679.
[53] Emad N, Yousif E, Ahmed D S, et al. Synthesis, physical properties, and carbon dioxide uptake of new metal-sulfamethoxazole complexes. Results in Chemistry, 2021, 6: 101137.
[54] House K, Baclig A, Ranjan M, et al. Economic and energetic analysis of capturing CO_2 from ambient air. Proceedings of the National Academy of Sciences, 2011, 108(51): 20428–20433.
[55] Derevschikov V S, Veselovskaya J V, Kardash T Y, et al. Direct CO_2 capture from ambient air using K_2CO_3/Y_2O_3 composite sorbent. Fuel, 2014, 127: 212–218.
[56] Goldberg D S, Lackner K S, Han P, et al. Co-location of air capture, subseafloor CO_2 sequestration, and energy production on the Kerguelen plateau. Environmental Science & Technology, 2013, 47(13): 7521–7529.
[57] Li H G, Zick M E, Trisukhon T, et al. Capturing carbon dioxide from air with charged-sorbents. Nature, 2022, 630(8017): 654–659.
[58] Castro P S, Bhattacheryyya S, Yadav R M, et al. A comprehensive overview of carbon dioxide capture: From materials, methods to industrial status. Materials Today, 2022, 60: 227–270.
[59] Fasihi M, Efimova O, Breyer C. Techno-economic assessment of CO_2 direct air capture plants. Journal of Cleaner Production, 2019, 224: 957–980.
[60] Wang X X, Song C S. Capture of CO_2 from concentrated sources and the atmosphere. In: An Economy Based On Carbon Dioxide and Water. Springer, 2019: 23–56.
[61] Elfving J, Bajamundi C, Kauppinen J, et al. Modelling of equilibrium working capacity of PSA, TSA and TVSA processes for CO_2 adsorption under direct air capture conditions. Journal of CO_2 Utilization, 2017, 22: 270–277.

[62] Mahmoudkani M, Keith D W. Low-energy sodium hydroxide recovery for CO_2 capture from atmospheric air-thermodynamic analysis. International Journal of Greenhouse Gas Control, 2009, 3(4): 376–384.